Optics Letters

Polarization-preserving image rotator

Suman Karan,[1,*] Aman Srivastava,[2] Pratham Sachin Todkar,[2] and Anand K. Jha[1,3]

[1] Department of Physics, Indian Institute of Technology Kanpur, Kanpur, UP 208016, India
[2] Department of Computer Science and Engineering, Indian Institute of Technology Kanpur, Kanpur, UP 208016, India
[3] akjha@iitk.ac.in
*sumankaran2@gmail.com

Received 21 April 2026; revised 14 July 2026; accepted 23 July 2026; posted 24 July 2026; published 7 August 2026

A K-mirror rotates the wavefront of an incident optical field. However, the rotation always introduces polarization changes in the transmitted field. This is a serious concern for applications ranging from astronomical image derotation to orbital angular momentum characterization in photonic quantum technology. Recent efforts have provided ways to minimize polarization changes, but these require either a very small base angle that limits the field of view, or mirrors with a customized refractive index. Nonetheless, image rotation without any associated polarization change has remained an open problem. In this work, we show that placing half-wave plates before and after a K-mirror and rotating them synchronously at half the K-mirror rotation angle makes the polarization change in the transmitted field completely independent of the rotation angle. Using a K-mirror with a base angle of 30°, which gives the largest field of view among practical designs, we experimentally demonstrate this, within the mean polarization error of ∼1% caused mostly by the retardance error of commercially available half-wave plates. Our scheme works at any base angle and mirror refractive index. More importantly, it works not only for K-mirrors but also for any type of image rotator. Thus, it can have important implications for applications requiring precise wavefront rotation without polarization change.

https://doi.org/10.1364/OL.603319

Rotating the wavefront of an optical field is always accompanied by polarization changes in the transmitted field [1,2]. This is a fundamental challenge in applications ranging from astronomy to high-dimensional orbital angular momentum (OAM) based quantum optics [3,4]. In astronomical telescopes, image rotators are used as image derotators in alt-azimuth mounts to counteract image rotation during sky tracking [5]. The rotation-dependent polarization change affects polarimetric and coronagraphic measurements [6–8]. In quantum optical experiments, wavefront rotation is central to OAM spectrum characterization via angular coherence measurement of optical fields, both at the high-light [9–12] and single-photon levels [3,13,14]. Any rotation-induced polarization change directly compromises the interferometric visibility and therefore the measurement fidelity [4,14]. Apart from these applications, image rotators find use in a broad range of other optical systems, including interferometry [15,16], microscopy [17], pattern recognition [18], and holography [19]. Among the various devices used for wavefront rotation [1,3,20], K-mirrors are most suitable [2,21]. They consist of three mirrors with independent controls and can be aligned to yield angular deviations of less than 200 microradians due to rotation, which is an order of magnitude lower than what is possible with other commercially available image rotators [21].

Efforts have been made to reduce the polarization change induced by a rotating K-mirror from 30−50% for a commercially available K-mirror [2] to as low as 3−10% [22]. However, these approaches have major limitations. With commercially available mirror coatings, a near-zero polarization change requires a small base angle of 17.88°, which significantly reduces the field of view [22]. On the other hand, at the base angle of 30°, which gives the largest field of view, mirrors with customized refractive indices are required. Thus, currently, there is no viable scheme for rotating a wavefront for which the associated polarization change is completely independent of the rotation angle.

In this work, we show that placing half-wave plates (HWP) before and after a K-mirror and rotating them synchronously at half the K-mirror rotation angle makes the transmitted polarization state completely independent of the rotation angle. We refer to this device as a polarization-preserving image rotator (PPIR). We present a Jones matrix analysis that analytically establishes this result. This scheme works for any base angle, mirror refractive index, or input state of polarization. We further show that our scheme for achieving polarization-preserving image rotation is universal and works not only for a K-mirror but also for any other image rotator. We experimentally demonstrate this using a home-built K-mirror with a base angle of 30°. This gives the largest field of view among practical designs. For three different input states of polarization, namely linear, elliptical, and circular, we report mean polarization errors of ∼1%, caused mostly by the retardance errors of the commercially available half-wave plates.

Figure 1 shows the design of our PPIR device, which consists of a K-mirror with two half-wave plates, HWP_1 and HWP_2, placed before and after it, respectively. All three components are mounted on a common rotation stage driven by a stepper motor, such that the HWPs rotate synchronously by $\theta/2$ when the K-mirror is rotated by θ. In order to analyze the transmitted states of polarization, we use the Jones matrix formalism. The incident electric field is written as $\boldsymbol{E}^{\text{in}} = E_x^{\text{in}}\,\hat{\boldsymbol{x}} + E_y^{\text{in}}\,\hat{\boldsymbol{y}}$, where $E_x^{\text{in}} = \cos\psi_{\text{in}}$ and $E_y^{\text{in}} = \sin\psi_{\text{in}} e^{i\delta_{\text{in}}}$. The Jones matrix of the

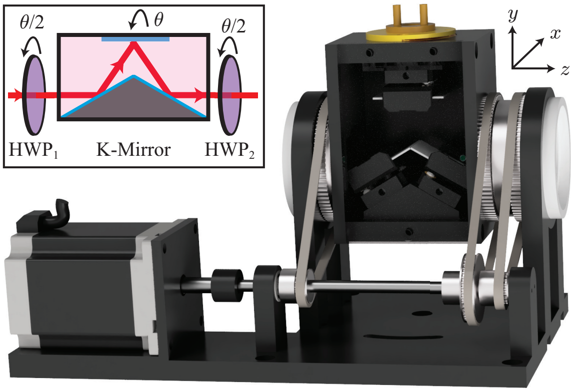

Fig. 1. Three-dimensional model of the home-built polarization-preserving image rotator (PPIR) device for wavefront rotation. It consists of a K-mirror with two half-wave plates (HWP), HWP$_1$ and HWP$_2$, placed before and after the K-mirror, respectively. Both HWPs and the K-mirror are mounted on a common rotation stage driven by a stepper motor. The HWPs rotate at half the rotation angle of the K-mirror. The inset shows the conceptual schematic.

K-mirror at rotation angle θ as given in Ref. [2], is:

$$t_{\mathrm{KM}}(\theta)=\begin{bmatrix} t^s_{\mathrm{KM}}\cos^2\theta+t^p_{\mathrm{KM}}\sin^2\theta & \left(t^s_{\mathrm{KM}}-t^p_{\mathrm{KM}}\right)\sin\theta\cos\theta \\ \left(t^s_{\mathrm{KM}}-t^p_{\mathrm{KM}}\right)\sin\theta\cos\theta & t^p_{\mathrm{KM}}\cos^2\theta+t^s_{\mathrm{KM}}\sin^2\theta \end{bmatrix}, \tag{1}$$

where $\theta=0^\circ$ is defined when all three mirrors of the K-mirror are in the $\boldsymbol{xz}$ plane. t^s_{KM} and t^p_{KM} are the complex amplitude transmission coefficients of the K-mirror for the s- and p-polarization components, respectively; their explicit forms in terms of the base angle β of the K-mirror and the refractive index n_M of the mirror coating are given in Refs. [2,22]. For a half-wave plate with retardance $\pi+\epsilon$, where ϵ is the retardance error, the Jones matrix with the fast axis at angle $\theta/2$ with respect to $\hat{x}$ can be expressed as:

$$\mathrm{HWP}^{\epsilon}(\theta)=\begin{bmatrix} \cos^2\theta-e^{i\epsilon}\sin^2\theta & \left(1+e^{i\epsilon}\right)\sin\theta\cos\theta \\ \left(1+e^{i\epsilon}\right)\sin\theta\cos\theta & \sin^2\theta-e^{i\epsilon}\cos^2\theta \end{bmatrix}. \tag{2}$$

If the retardance errors of HWP$_1$ and HWP$_2$ are ϵ_1 and ϵ_2, respectively, the Jones matrix of the PPIR at rotation angle θ can be written as:

$$t_{\mathrm{PPIR}}(\theta)=\mathrm{HWP}_2^{\epsilon_2}(\theta/2)\times t_{\mathrm{KM}}(\theta)\times\mathrm{HWP}_1^{\epsilon_1}(\theta/2). \tag{3}$$

The transmitted field $\boldsymbol{E}^{\mathrm{out}}=E^{\mathrm{out}}_x\,\hat{x}+E^{\mathrm{out}}_y\,\hat{y}$ at any rotation angle θ of the PPIR is given by $\boldsymbol{E}^{\mathrm{out}}=t_{\mathrm{PPIR}}(\theta)\boldsymbol{E}^{\mathrm{in}}$. For ideal half-wave plates, $\epsilon_1=\epsilon_2=0$, and Eq. (3) reduces to:

$$t_{\mathrm{PPIR}}(\theta)=\begin{bmatrix} t^s_{\mathrm{KM}} & 0 \\ 0 & t^p_{\mathrm{KM}} \end{bmatrix}, \tag{4}$$

where $t_{\mathrm{PPIR}}(\theta)$ is independent of θ, and thus the transmitted state of polarization is completely independent of the rotation angle. This holds for any base angle, any mirror refractive index, and any input state of polarization. From Eq. (4), we infer that for a horizontally (H) polarized input state $[1,0]^{\mathrm{T}}$, the transmitted states for any arbitrary θ are $[t^s_{\mathrm{KM}},0]^{\mathrm{T}}$, and for a vertically (V) polarized input state $[0,1]^{\mathrm{T}}$, the transmitted states are $\left[0,t^p_{\mathrm{KM}}\right]^{\mathrm{T}}$. Since t^s_{KM} and t^p_{KM} are just two complex numbers,

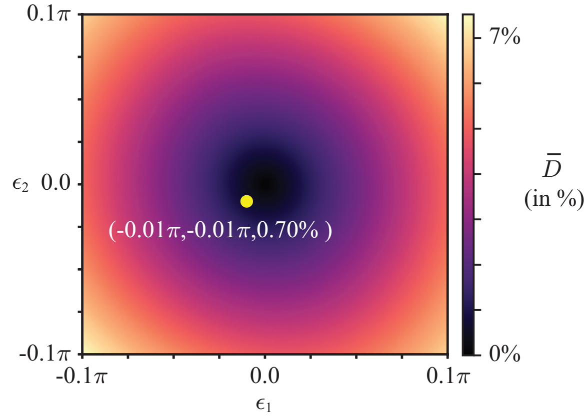

Fig. 2. Numerically simulated plot of mean polarization errors $\bar{D}$ in % as a function of the retardance errors ϵ_1 and ϵ_2 of HWP1 and HWP2, respectively, for a linearly polarized input state. The yellow dot marks the operating point corresponding to commercially available Thorlabs HWPs.

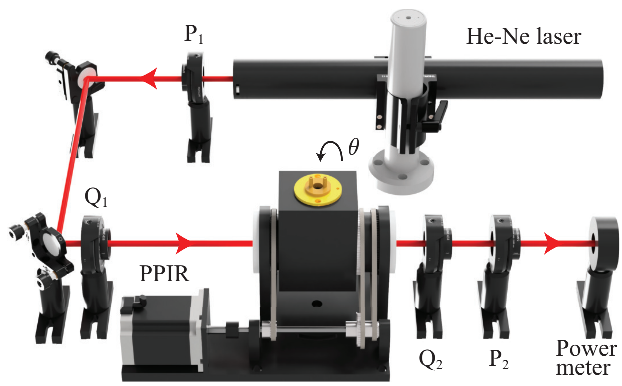

Fig. 3. Schematic of the experimental setup to measure the transmitted state of polarization at different rotation angles of the polarization-preserving image rotator (PPIR) device. P_1, P_2: polarizers; Q_1, Q_2: quarter-wave plates.

they have no effect on the polarization state, and thereby the transmitted states are the same as the respective input states. We note that for input states of polarization (SOP) other than these two special cases, the transmitted SOP will not be the same as the incident state. We further note that the above scheme is universal in the sense that it achieves polarization-preserving image rotation not only for a K-mirror but also for any image rotator (see Supplement 1).

The state of polarization of $\boldsymbol{E}^{\mathrm{in(out)}}$ can be uniquely represented by four Stokes parameters: $S_0^{\mathrm{in(out)}}=|E_x^{\mathrm{in(out)}}|^2+|E_y^{\mathrm{in(out)}}|^2$, $S_1^{\mathrm{in(out)}}=|E_x^{\mathrm{in(out)}}|^2-|E_y^{\mathrm{in(out)}}|^2$, $S_2^{\mathrm{in(out)}}=2\mathrm{Re}\left[E_x^{\mathrm{in(out)}*}E_y^{\mathrm{in(out)}}\right]$, and $S_3^{\mathrm{in(out)}}=2\mathrm{Im}\left[E_x^{\mathrm{in(out)}*}E_y^{\mathrm{in(out)}}\right]$ [23]. Here * denotes the complex conjugation. For a state with degree of polarization equal to 1, the normalized Stokes parameters are: $\bar{S}_1^{\mathrm{in(out)}}=S_1^{\mathrm{in(out)}}/S_0^{\mathrm{in(out)}}$, $\bar{S}_2^{\mathrm{in(out)}}=S_2^{\mathrm{in(out)}}/S_0^{\mathrm{in(out)}}$, and $\bar{S}_3^{\mathrm{in(out)}}=S_3^{\mathrm{in(out)}}/S_0^{\mathrm{in(out)}}$. These normalized Stokes parameters $\left(\bar{S}_1^{\mathrm{in(out)}},\bar{S}_2^{\mathrm{in(out)}},\bar{S}_3^{\mathrm{in(out)}}\right)$ can be represented as a point on the surface of the Poincaré sphere, where each point uniquely represents a particular state of polarization.

Ideally, if the transmitted state is completely rotation-independent, all states measured at rotation angles from 0° to

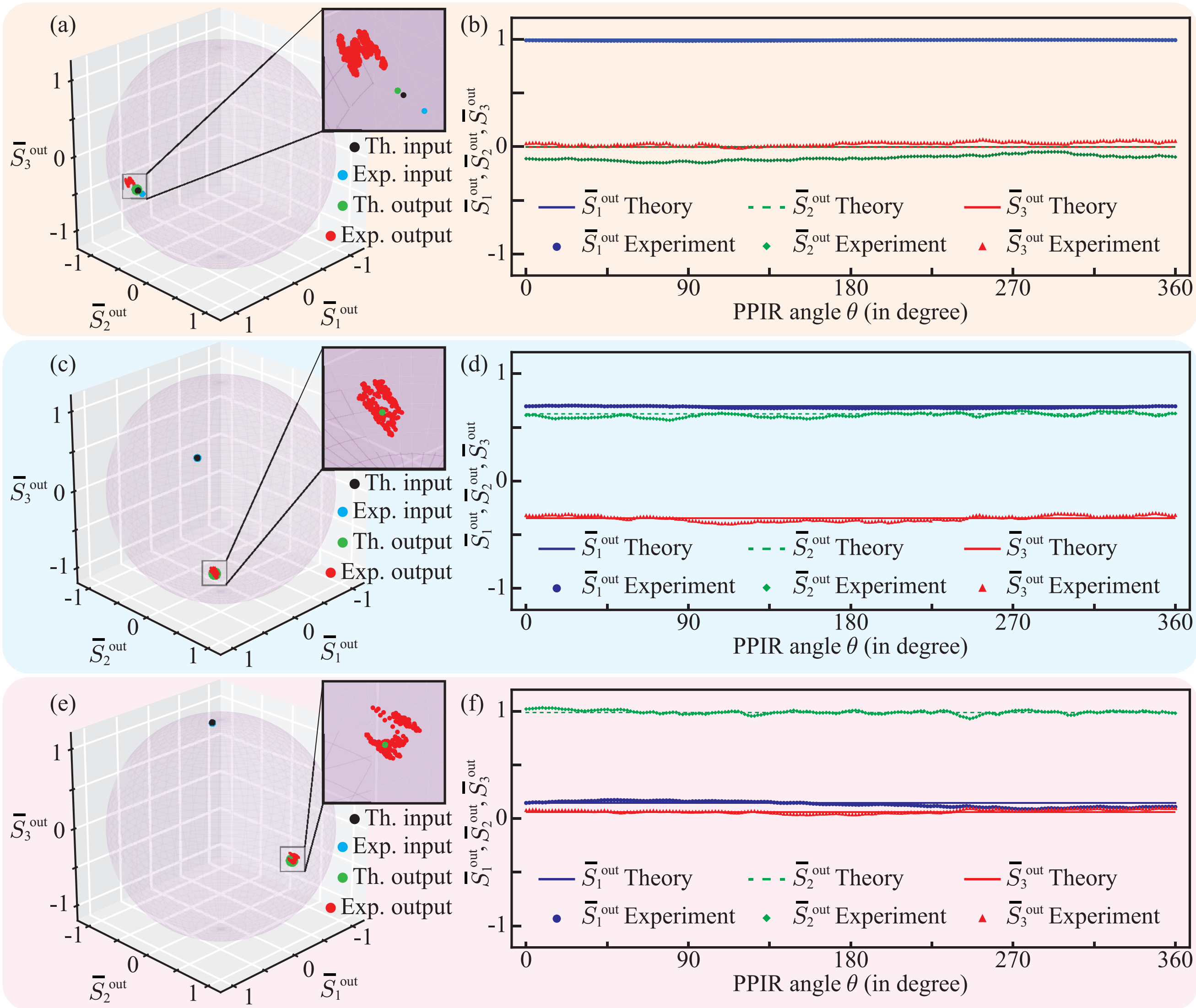

Fig. 4. Poincaré sphere representation of the transmitted SOP at different rotation angles of the PPIR device for three different input states of polarization: (a) linear, (c) elliptical, and (e) circular. The corresponding normalized Stokes parameters are shown in (b), (d), and (f), respectively. In each case, the insets show a magnified view of the theoretically expected (green dots) and experimentally observed (loops consisting of red dots) transmitted states of polarization.

360° map to a single point on the surface of the Poincaré sphere. Otherwise, they form a loop, as shown in Ref. [2]. The smaller the loop, the smaller the polarization change due to rotation. As Eq. (4) shows, the Jones matrix of the PPIR has no θ dependence, and therefore the transmitted SOP maps to a single point on the Poincaré sphere.

Inspired by the metric defined in Ref. [2], we define the mean polarization error $\bar{D}$ as the mean geodesic distance on the surface of the Poincaré sphere between the transmitted state of polarization at $\theta = 0°$ and the transmitted SOP at all other rotation angles θ of PPIR. We express $\bar{D}$ in percent form as:

$$\bar{D} = \frac{\int_{\theta=0}^{2\pi} \cos^{-1}\left[\sum_{i=1}^{3} \bar{S}_i^{\text{out}}\, \bar{S}_i^{\text{out0}}\right] \sqrt{\sum_{i=1}^{3}\left(\frac{dS_i^{\text{out}}}{d\theta}\right)^2}\, d\theta}{\int_{\theta=0}^{2\pi}\sqrt{\sum_{i=1}^{3}\left(\frac{dS_i^{\text{out}}}{d\theta}\right)^2}\, d\theta}\,\%, \qquad \textbf{(5)}$$

where $\bar{S}_i^{\text{out0}}$, with $i \in \{1, 2, 3\}$ are the normalized Stokes parameters of the transmitted state of polarization at $\theta = 0°$. When the transmitted SOPs are completely rotation-independent, they map to a single point on the Poincaré sphere. In this case, Eq. (5) takes the 0/0 form, and from continuity we define $\bar{D}$ as 0%. Here, $\bar{D} = 0\%$ represents SOP completely independent of rotation, and $\bar{D} = 100\%$ corresponds to the maximum possible polarization change due to rotation.

Figure 2 shows the plot of numerically simulated $\bar{D}$ as a function of the retardance errors ϵ_1 and ϵ_2 of HWP1 and HWP2, respectively. Here, both ϵ_1 and ϵ_2 range from -0.1π to 0.1π. This shows $\bar{D} = 0\%$ for $\epsilon_1 = \epsilon_2 = 0$, and $\bar{D}$ increases as the retardance errors increase, in a manner consistent with a parabolic dependence on ϵ_1 and ϵ_2 near the origin. Although $\bar{D} = 0$ for ideal HWPs (see Eq. (4)), we use Thorlabs (WPHSM05-633) HWPs, with a manufacturer-specified retardance error of $\epsilon_1 = \epsilon_2 = -0.01\pi$. This leads to a theoretically expected $\bar{D}$ of 0.70%, represented by the yellow dot in Fig. 2.

Figure 3 shows the experimental setup for measuring the Stokes parameters of the transmitted SOP at different rotation angles θ of the PPIR and thereby for measuring $\bar{D}$. A 5 mW Newport He–Ne laser of wavelength 632.8 nm is sent through a linear polarizer P_1 to generate H-polarized light. We then insert a quarter-wave plate Q_1 with its fast axis rotated at 24° and 45° to generate elliptically and circularly polarized input states, respectively. We note that Q1 is placed close to the K-mirror in order to minimize any reflection-related polarization changes to the input field. In assembling our home-built PPIR, we use Thorlabs 1 inch protected silver mirrors PF10-03-P01 and zero-order half-wave plates WPHSM05-633 as HWP_1 and HWP_2. The image rotator is aligned such that the angular deviation of the light beam passing through it is less than a milliradian, which also ensures that the light field is incident normally on the two half-wave plates to within a milliradian. Using standard Stokes parameter measurement via polarizer P_2, quarter-wave plate Q_2, and a power meter, we measure the transmitted SOP at different rotation angles θ of the PPIR.

Figure 4 presents the experimental results. The Poincaré sphere representation of the experimentally measured transmitted SOP for rotation angles θ from 0° to 360° in steps of 1.8° for a linearly polarized incident state of polarization is shown in Fig. 4(a). The theoretical incident polarization state is denoted by a black dot on the Poincaré sphere. The experimentally measured incident state of polarization is shown by the blue dot. The theoretically predicted transmitted SOPs are shown by the green dot, and the corresponding experimentally measured SOPs are shown by the red loop. The inset shows a magnified view of these loops. Figure 4(b) shows the theoretically expected and experimentally measured normalized Stokes parameters: $\bar{S}_1^{\mathrm{out}}$, $\bar{S}_2^{\mathrm{out}}$, and $\bar{S}_3^{\mathrm{out}}$ as a function of θ for the same linearly polarized input state. The corresponding plots for the elliptically and circularly polarized incident SOP are shown in Figs. 4(c)–4(f), respectively. The measured mean polarization errors for linearly, elliptically, and circularly polarized input states are 0.96%, 1.18%, and 1.01%, respectively, all consistent with the theoretically predicted value of 0.70%.

In conclusion, we have proposed and demonstrated a polarization-preserving image rotator (PPIR) that rotates a wavefront while keeping the transmitted state of polarization completely independent of the rotation angle. The PPIR consists of a K-mirror placed between two HWPs, assembled such that when the K-mirror is rotated by θ, the HWPs rotate by $\theta/2$. We have demonstrated that for protected silver mirror coating and a base angle of 30°, which gives the largest field of view, the mean polarization error is only ∼1% for linearly, elliptically, and circularly polarized input states. This is primarily due to the retardance error of the commercially available HWPs, with additional contributions from experimental imperfections such as small misalignments and imperfect preparation of the input polarization state. We have also shown that for H- and V-polarized input states, the transmitted SOP not only remains the same for all rotation angles but also coincides with the input state of polarization, which could be very useful for interferometry-based applications [4,14]. Furthermore, we have shown that our scheme is universal and that it works for any image rotator, not just the K-mirror. Our work can have significant implications for image derotation and orbital angular momentum-based high-dimensional quantum information applications where achieving wavefront rotation without polarization change is very crucial.

Funding. Science and Engineering Research Board (CRG/2022/003070); Department of Science and Technology (DST/ICPS/QuST/Theme-1/2019, DST/FFT/NQM/QSM/2024/3).

Acknowledgment. The authors thank M. P. Van Exter for useful discussions and Inesh Aggarwal for his contribution in the initial implementation of the scheme.

Disclosures. The authors declare no conflicts of interest.

Data availability. Data underlying the results presented in this paper are not publicly available at this time but may be obtained from the authors upon reasonable request.

Supplemental document. See Supplement 1 for supporting content.

REFERENCES

1. I. Moreno, Appl. Opt. **43**, 3373 (2004).
2. S. Karan, P. Mohta, A. K. Jha, *et al.*, Appl. Opt. **61**, 8302 (2022).
3. J. Leach, J. Courtial, K. Skeldon, *et al.*, Phys. Rev. Lett. **92**, 013601 (2004).
4. H. Di Lorenzo Pires, H. C. B. Florijn, and M. P. van Exter, Phys. Rev. Lett. **104**, 020505 (2010).
5. P. Guo, J. Zhang, F. Yang, *et al.*, in *7th International Symposium on Advanced Optical Manufacturing and Testing Technologies: Large Mirrors and Telescopes*, vol. **9280** (SPIE, 2014), p. 92800C.
6. H. M. Schmid, A. Bazzon, R. Roelfsema, *et al.*, Astron. Astrophys. **619**, A9 (2018).
7. R. G. van Holstein, C. U. Keller, F. Snik, *et al.*, Astron. Astrophys. **677**, A150 (2023).
8. R. M. Anche, J. N. Ashcraft, S. Y. Haffert, *et al.*, Astron. Astrophys. **672**, A121 (2023).
9. F.-X. Wang, W. Chen, Y.-P. Li, *et al.*, Opt. Express **25**, 24946 (2017).
10. N. González, G. Molina-Terriza, and J. P. Torres, Opt. Express **14**, 9093 (2006).
11. H. D. L. Pires, J. Woudenberg, and M. P. van Exter, Opt. Lett. **35**, 889 (2010).
12. G. Kulkarni, S. Karan, and A. K. Jha, Phys. Rev. Appl. **13**, 054077 (2020).
13. J. Leach, M. J. Padgett, S. M. Barnett, *et al.*, Phys. Rev. Lett. **88**, 257901 (2002).
14. S. Karan, M. P. Van Exter, and A. K. Jha, Sci. Adv. **11**, eadq7201 (2025).
15. S.-C. Chu, C.-S. Yang, and K. Otsuka, Opt. Express **16**, 19934 (2008).
16. R. Mohanty, C. Joenathan, and R. Sirohi, Opt. Commun. **47**, 27 (1983).
17. Y. Zhi, R. Lu, B. Wang, *et al.*, Opt. Lett. **40**, 1683 (2015).
18. H. Fujii and Y. Ohtsuka, Opt. Commun. **36**, 255 (1981).
19. C. Pérez-López, F. M. Santoyo, G. Pedrini, *et al.*, Appl. Opt. **40**, 5106 (2001).
20. M. J. Padgett and J. P. Lesso, J. Mod. Opt. **46**, 175 (1999).
21. W. H. Peeters, E. J. K. Verstegen, and M. P. van Exter, Phys. Rev. A **76**, 042302 (2007).
22. S. Karan, N. Senapati, and A. K. Jha, Appl. Opt. **63**, 4552 (2024).
23. D. H. Goldstein, *Polarized Light* (CRC Press, 2017).